Accepted Manuscript

Cytotoxicity, molecular modeling, cell cycle arrest, and apoptotic induction induced by novel tetrahydro-[1,2,4]triazolo[3,4-*a*]isoquinoline chalcones

Magda F. Mohamed, Hamdi M. Hassaneen, Ismail A. Abdelhamid

PII: S0223-5234(17)30948-0

DOI: 10.1016/j.ejmech.2017.11.045

Reference: EJMECH 9920

To appear in: *European Journal of Medicinal Chemistry*

Received Date: 25 May 2017

Revised Date: 5 November 2017

Accepted Date: 17 November 2017

Please cite this article as: M.F. Mohamed, H.M. Hassaneen, I.A. Abdelhamid, Cytotoxicity, molecular modeling, cell cycle arrest, and apoptotic induction induced by novel tetrahydro-[1,2,4]triazolo[3,4-*a*]isoquinoline chalcones, *European Journal of Medicinal Chemistry* (2017), doi: 10.1016/j.ejmech.2017.11.045.

Graphical Abstract

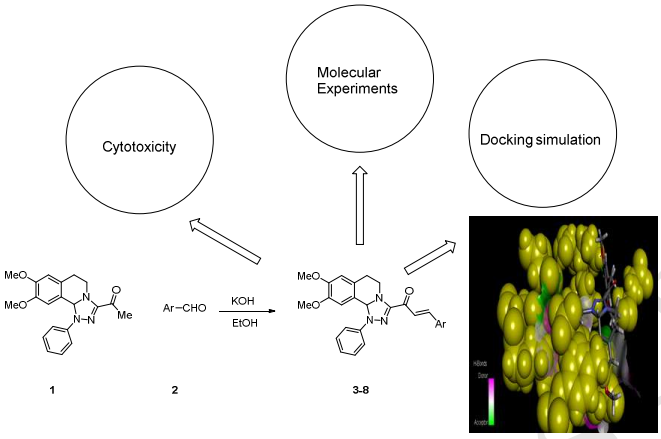

Cytotoxicity, molecular modeling, cell cycle arrest, and apoptotic induction induced by novel tetrahydro-[1,2,4]triazolo[3,4-*a*]isoquinoline chalcones

Magda F. Mohamed,[a*] Hamdi M. Hassaneen [b] and Ismail A. Abdelhamid [b*]

[a] Department of Chemistry (Biochemistry Branch), Faculty of Science, Cairo University, Giza, Egypt, magdafikry85@yahoo.com

[b] Department of Chemistry, Faculty of Science, Cairo University, Giza, Egypt. ismail_shafy@yahoo.com

Abstract

Novel tetrahydro-[1,2,4]triazolo[3,4-*a*]isoquinolin-3-yl)-3-arylprop-2-en-1-one derivatives were synthesized and their structures were confirmed by different spectral tools. Cytotoxicity test revealed that some compounds exhibited strong to moderate effect, while others showed weak action against different cancer cell lines (MCF7, A549, HCT116, and Hepg2). Breast carcinoma revealed higher sensitivity toward all derivatives especially compounds **5** and **8** which offered the lowest IC_{50} values (50.05, and 27.15 µg/ml) respectively, relative to the positive control 5-fluorouracil (5-FU) (IC_{50} = 178 µg/ml). In addition, the two compounds exhibited less toxic effect toward normal melanocytes (HFB4). Several theoretical and experimental studies were done to reveal the molecular mechanisms that control breast carcinoma metastasis using the two promising novels **5** and **8**. Docking simulation studies against the two proteins EGFR and DHFR demonstrate that compound **8** showed higher binding affinity toward the two proteins more than compound **5**, suggesting that trimethoxy groups may be responsible for this higher activity through the formation of five hydrogen bonding with the active domain (4r3r) and other four interactions with the active domain (1dls). Real time PCR assay illustrates that the two compounds up regulated BAX, p53, caspase-3 genes and down regulated BCL2, MMP1, CDK4 ones. In addition, it was noted that compound **8** was more effective in gene regulation and apoptotic induction than compound **5.** Also, flow cytometer analysis demonstrates that both compounds **5** and **8** induced cell growth arrest at G1 phase and thus, inhibit G1/S transition and cell cycle progression. In addition, both compounds stimulate apoptotic death of breast cells significantly to reach 8.72%, and 17.28% respectively, compared to their control (0.55%). Apoptotic induction of breast cells was enhanced effectively through activation of caspase-3 by compound **8** using Elisa assay.

Keywords: Breast cancer, Modeling study, Apoptosis, Cell cycle arrest, Caspase-3, p53, tetrahydro-[1,2,4]triazolo[3,4-*a*]isoquinoline, chalcones.

1. Introduction

Chalcones are distinguished secondary metabolites that are reported to exhibit various bioactivities such as antiplatelet[1], antiviral[2], anti-inflammatory[3–5], antimalarial[6], antibacterial,[7,8]analgesic[9], anticancer[8,10–12], and antioxidant[4,10]. The presence of a reactive *a*,*ß*-unsaturated ketonic group in chalcone derivatives is considered to be responsible for their bioactivity. Moreover, heterocyclic compounds having nitrogen such as [l,2,4]triazolo[3,4-*a*]isoquinolines showed considerable pharmaceutical activities[13] such as anti-inflammatory[13], antidepressant[13] and cardiovascular[13]. These interesting biological activities have motivated us to synthesize the chalcones of the [l,2,4]triazolo[3,4-*a*]isoquinolines ring systems.

Epidermal growth factor receptor (EGFR) has been involved in different kinds of malignancies such as breast, pancreatic cancer, neck, and head. Various types of drugs have been established in order to block the tyrosine domain of EGFR as a target in cancer treatment[14–17]. Thus, a new series of tetrahydro[1,2,4]triazolo[3,4-*a*]isoquinoline chalcones were prepared and theoretically investigated by docking with the tyrosine domain EGFR, in trials to find new therapeutic agents which have promising and selective anticancer effect. In addition, another modeling study targeted the tumor marker DHFR enzyme which help DNA synthesis of tumor cell[18] has been performed. Moreover, this recent study has utilized different molecular techniques targeting to know the mechanism of action of the two strongly and promising derivatives **5** and **8** using breast carcinoma as an example.

2- Results and Discussion

2.1. Synthetic Chemistry

The starting 3-acetyl-8,9-dimethoxy-1-phenyl-1,5,6,10b-tetrahydro-[1,2,4]triazolo[3,4-*a*]isoquinoline **1** was obtained with high yields and purity following the reported procedures *via* the reactions of 3,4-dihydro-6,7-dimethoxyisoquinoline (**iii**) with

nitrilimines (**ii**) (Scheme 1)[13,19]. Claisen–Schmidt condensation of compound **1** with equimolar amounts of substituted aldehydes **2** in the presence of potassium hydroxide solution leads to the formation of the corresponding chalcone derivatives **3-8** (Scheme 2). The structures of the formed products were elucidated by inspection of their spectral data.

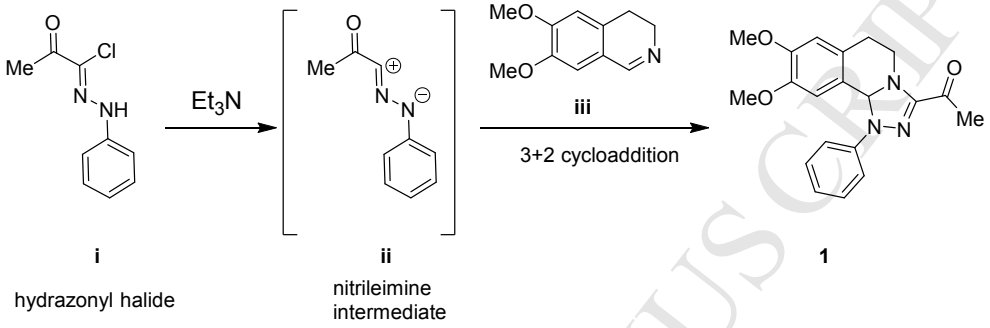

Scheme 1: Synthesis of 3-acetyl-8,9-dimethoxy-1-phenyl-1,5,6,10b-tetrahydro-[1,2,4]triazolo[3,4-*a*]isoquinoline **1**

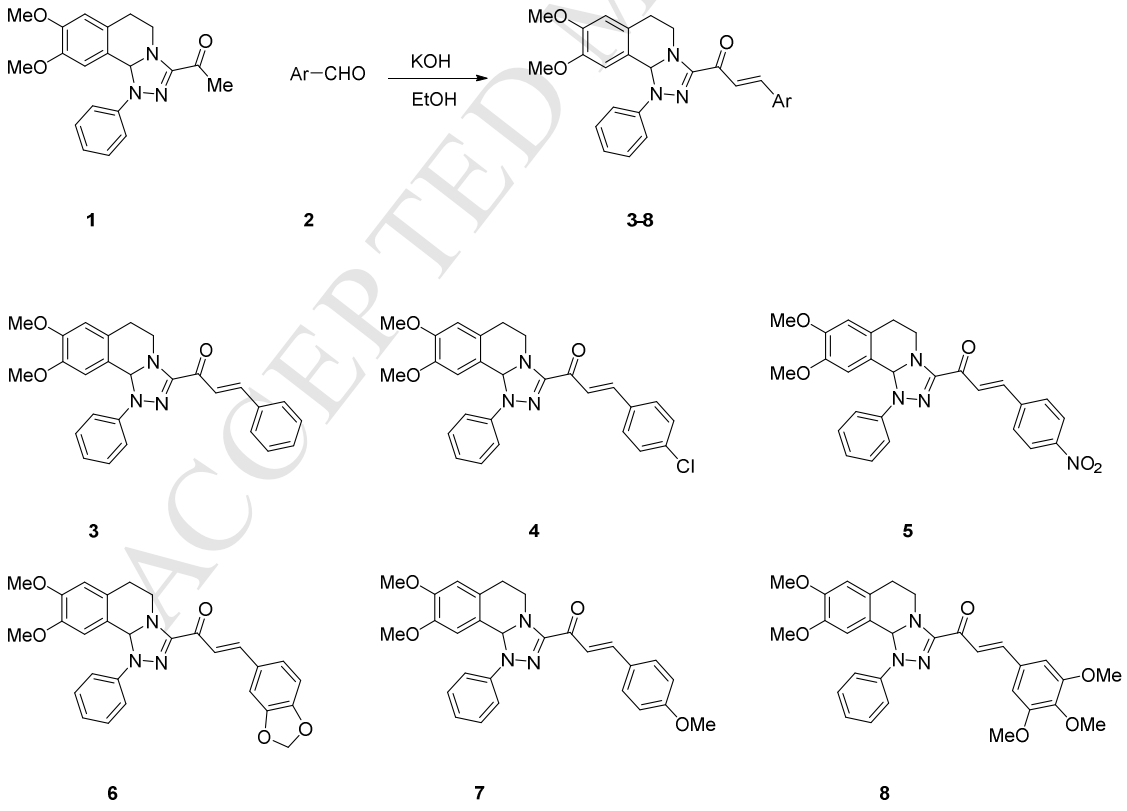

Scheme 2: Synthesis of tetrahydro-[1,2,4]triazolo[3,4-*a*]isoquinolin-3-yl)-3-arylprop-2-en-1-one (3-8)

MTT Assay

Cytotoxicity was performed on a novel series of tetrahydro[1,2,4]triazolo[3,4-*a*]isoquinoline chalcones derivatives **3-8**. The data obtained in Table 1 indicated that all compounds exhibited strong to weak effect against all selected cancer cell lines. Generally, breast carcinoma revealed higher and promising sensitivity with all prepared derivatives especially compounds **5** and **8** which offered the lowest IC_{50} values (50.05, and 27.15 µg/ml) respectively, relative to the positive control 5-fluorouracil (5-FU) with IC_{50} (178 µg/ml). This result concerning the most promising anticancer compound **8** was compatible to that obtained by Shenvi, *et al* [10] and Srivastava *et al* [20] where additional trimethoxy groups enhanced anticancer activity especially when compared to compound **4**. Compound **6** showed reduction in activity in case of MCF7. On the other hand, compounds **5** and **6** exhibited promising effect with colon carcinoma (114.2, and 187.4 µg/ml) respectively, compared to their control (201 µg/ml). Unfortunately, compounds **3, 4**, and **8** showed high IC_{50} values (weak effect) toward the same line. With respect to hepatocellular carcinoma (HEPG2), it was noted that all series exhibited better effect than 5-FU except compound **5** which exhibited moderate effect (as showed in Figure 1 and Table 1). Finally, compound **3** recorded strong effect with IC_{50} value (78.13 µg/ml) approximately near to that of 5-FU against lung carcinoma (A549) while the rest compounds showed moderate response regarding their standard control. Regarding their safety, all derivatives were tested for their toxic effect against human normal melanocytes (HFB4) (as showed in Table 1). It was found that compound **5** and **8** were the best ones where they exhibited low toxic effect against HFB4 cell line follow those in selectivity was compound **7,** while other compound showed high toxic effect. Compounds **5** and **8** were the best promising and selective anticancer drug especially against breast carcinoma thus, molecular studies were performed on these two compounds to know their mechanism in breast cancer inhibition.

Table 1: The IC_{50} values of the novel chalcones and the positive control 5-FU on human cell lines A549, MCF7, and HCT116, HEPG2, and normal melanocytes (HFB4).

Cell lines	IC_{50} Values (µg/ml) (the drug concentrations that inhibited 50 % of cell proliferation)						
	5FU	**3**	**4**	**5**	**6**	**7**	**8**
A549	66	78.13	155.7	206.82	201.41	189.90	156.30
MCF7	178	61.41	151.38	50.05	225.41	68.46	27.15
HCT116	201	625	622.3	114.2	187.4	243.2	NA
HEPG2	237	139.4	140.53	477.6	122.24	218.05	107.1
Normal melanocytes (HFB4)	-	52.1	57.2	245.15	51.9	115.07	No reading

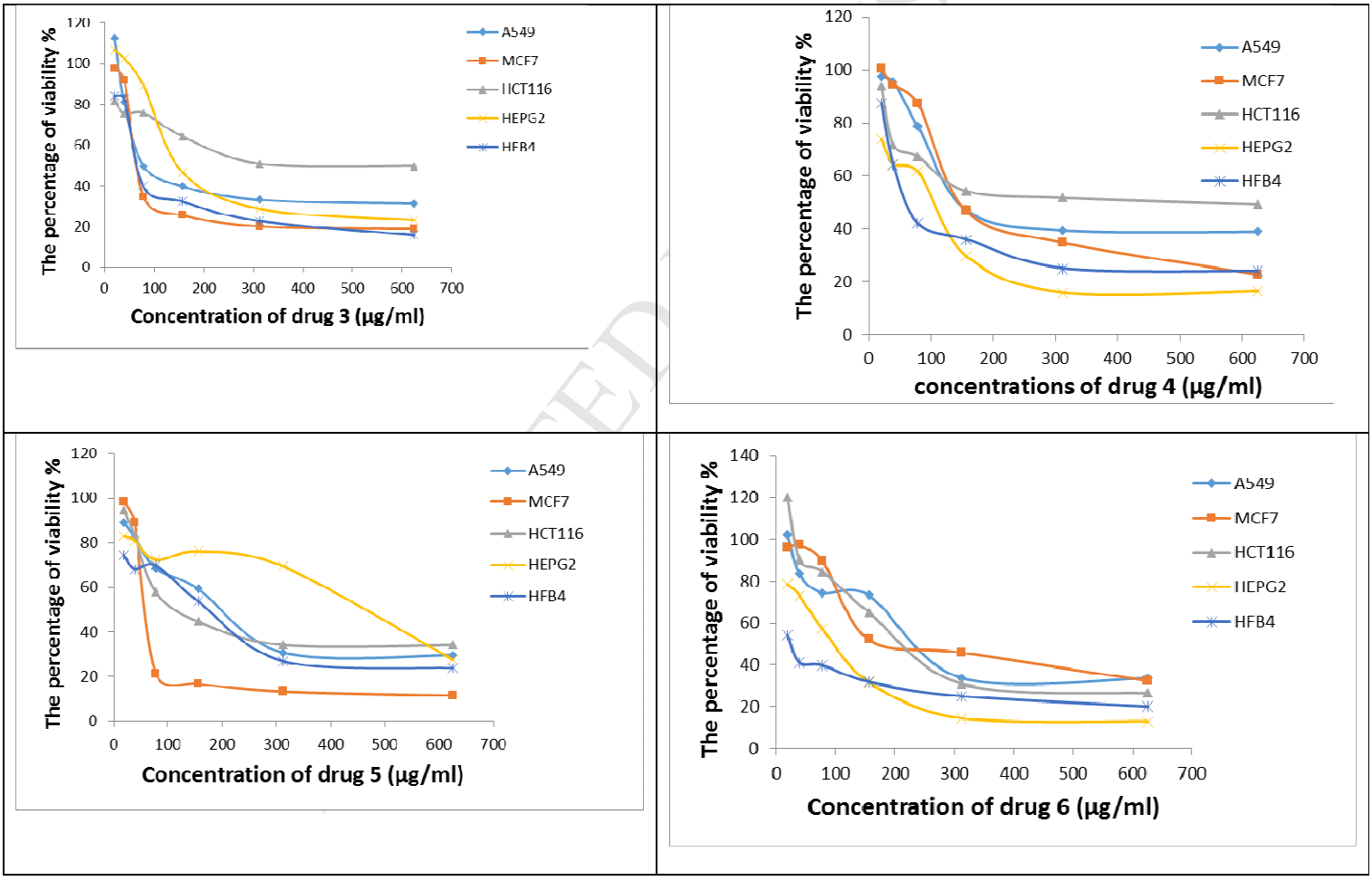

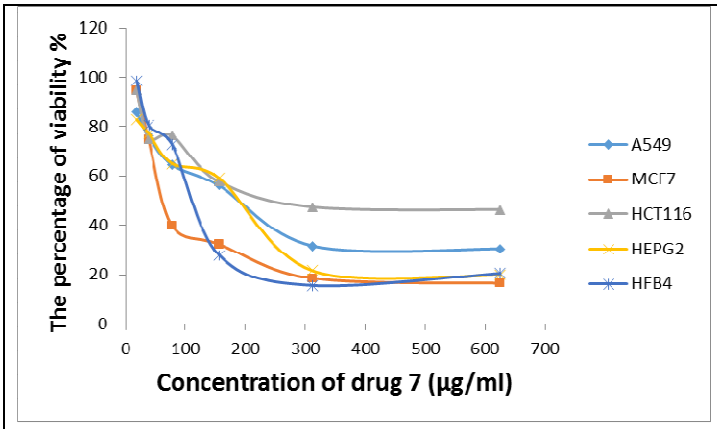

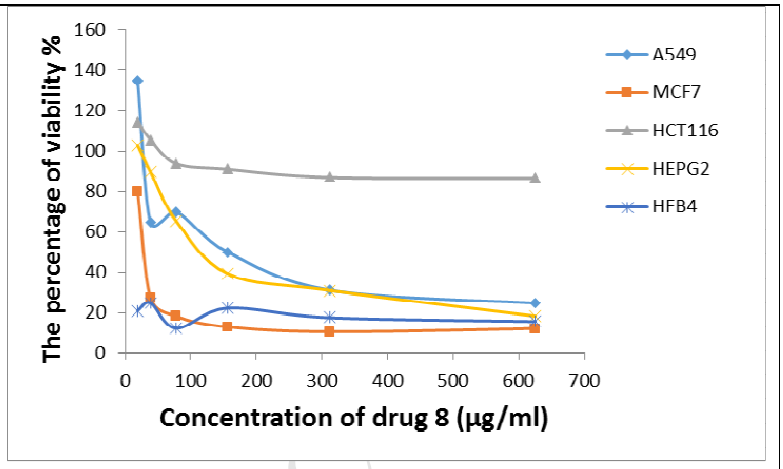

Figure 1: Cytotoxic evaluations of the tested compounds (**3-8**) against four tumor cell lines (A549, MCF7, HCT116, and HEPG2) and one tested normal line (HFB4) after 48 h of treatment using prism software program (Graphpad software incorporated, version 3).

Modeling Simulation Studies

Docking studies were used to predict the binding mode of ligand within the binding site of target proteins, to validate and specify the mechanism of action or proteins responsible for the anticancer activity. Cytotoxic activity of compounds **5** and **8** has been realized by using *in vitro* assay and proved the most active and promising chemotherapeutic agents. Accordingly, molecular modeling studies were performed against two human proteins which expressed in most of tumor cells especially breast carcinoma, the tyrosine domain of (EGFR) and dihydrofolate reductase enzyme (DHFR). Proteins were selected and downloaded from the Protein Data Bank (PDB ID: 4r3r, and 1dls) respectively. Proteins were optimized by removing water molecules and cofactors from the proteins, deleting the standard ligand present in the crystal structure. The bond order of the ligand and protein were adjusted. Target compounds were built using the chembiodraw ultra 10.0, protonate 3D and subjected to energy minimization. Docking studies of the most active compound **8** into the active domain 4r3r revealed five interactions with the three methoxy groups with different bond distances. Two interactions are between lys860 and two oxygen atoms of two methoxy with bond distances 2.4, and 2.37 A° respectively. The third and fourth interactions including Arg836 with two oxygen atoms with 2.6, and 2.19 A° respectively. The fifth one is between Arg858 and oxygen with bond distance

2.71 A° (as showed in Figure 2). It is suggested that the promising activity of compound **8** may be due to the presence of additional tri methoxy groups which enhanced the binding ability by five hydrogen interactions. Regarding the binding mode of compound **5** toward the same protein, it showed only two interactions, one of them is hydrogen bonding between lys875 and oxygen atom with bond distance 2.25 A° and the other binding is arene-cation interaction between benzene ring of *p*-nitrobenzene and lys879 (Figure 2). It is clear that the replacement of trimethoxy groups with nitrobenzene was not favored where the binding activity was decreased relative to compound **8**. With respect to DHFR enzyme, the two compounds were docked with the active domain (1dls) and also the results indicated that the binding mode of compound **8** was better than compound **5** (as showed in Figure 3). Compound **8** achieved four binding while one binding mode was achieved by compound **5**. Two interactions are hydrogen bonding between Arg28 and two oxygen. The other two modes were arene-arene interactions between each of the phenyl and trimethoxyphenyl rings with phe34 and phe31 respectively (Figure 3). All these binding modes confirmed our suggestion that trimethoxy group played an important role behind the enhanced binding activity of compound **8** into the active site of the target proteins and hence inhibit cancer progression.

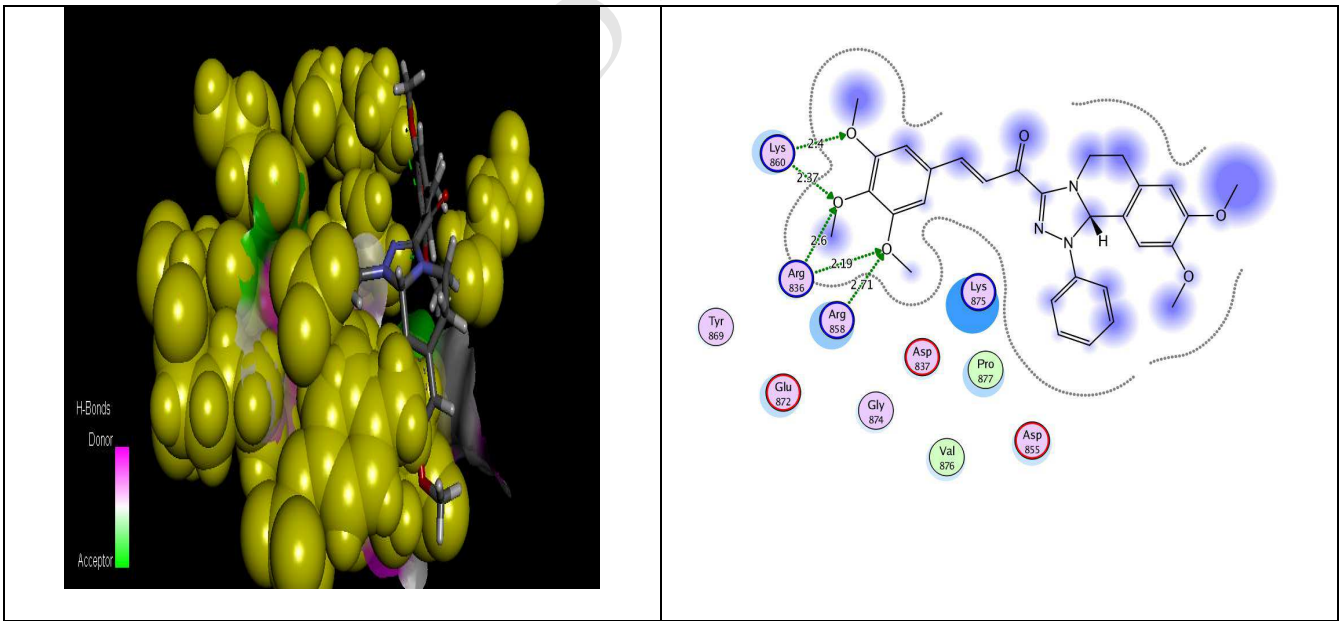

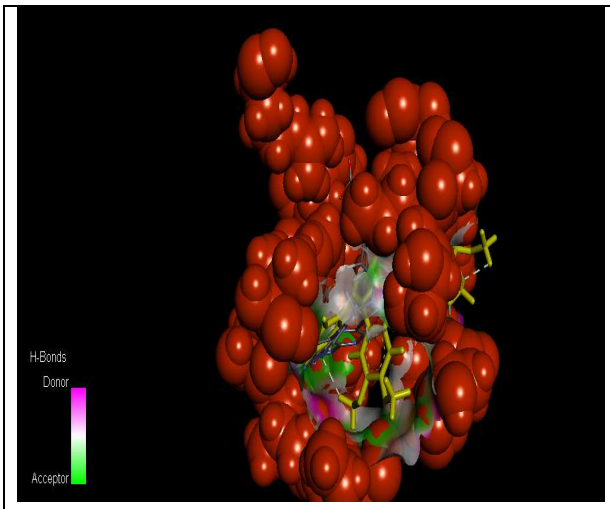

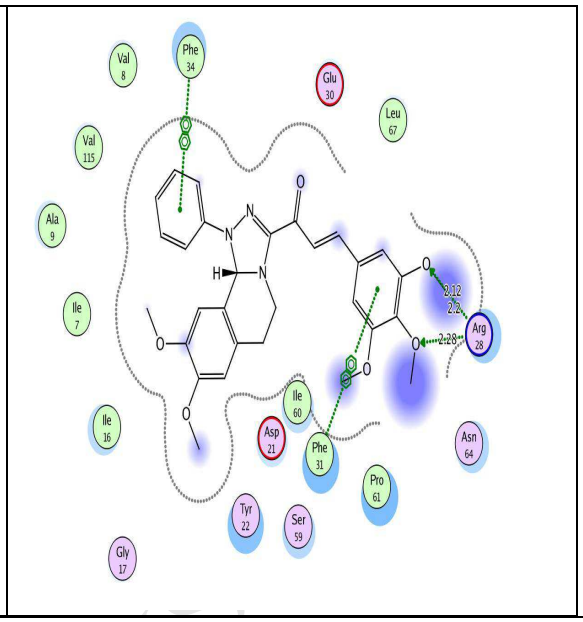

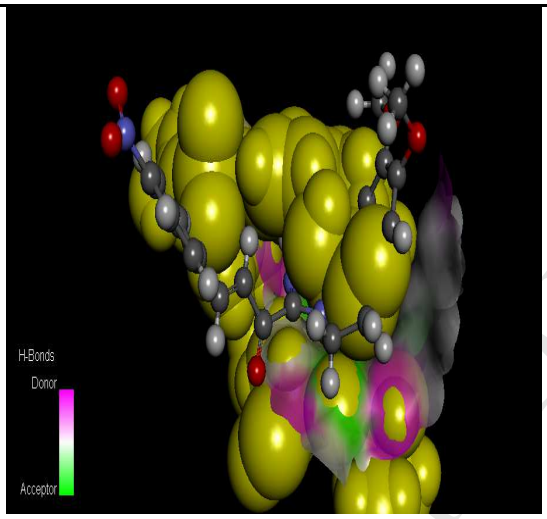

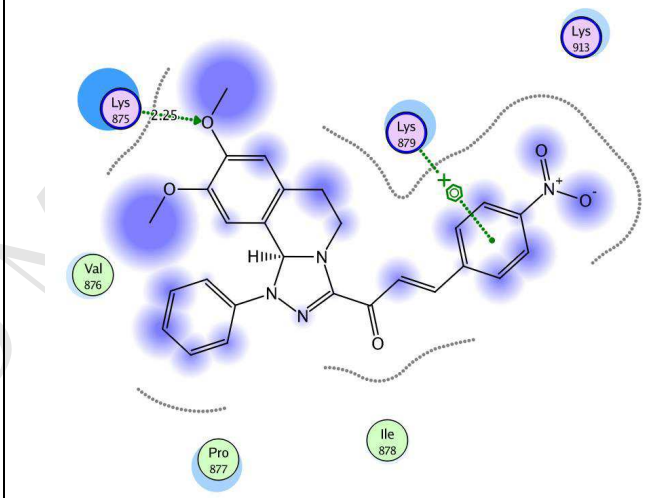

Figure 2: 3D and 2D dimensional representation of compounds **8** and **5** respectively, into the active site tyrosine kinas domain of human epidermal growth factor receptor (EGFR).

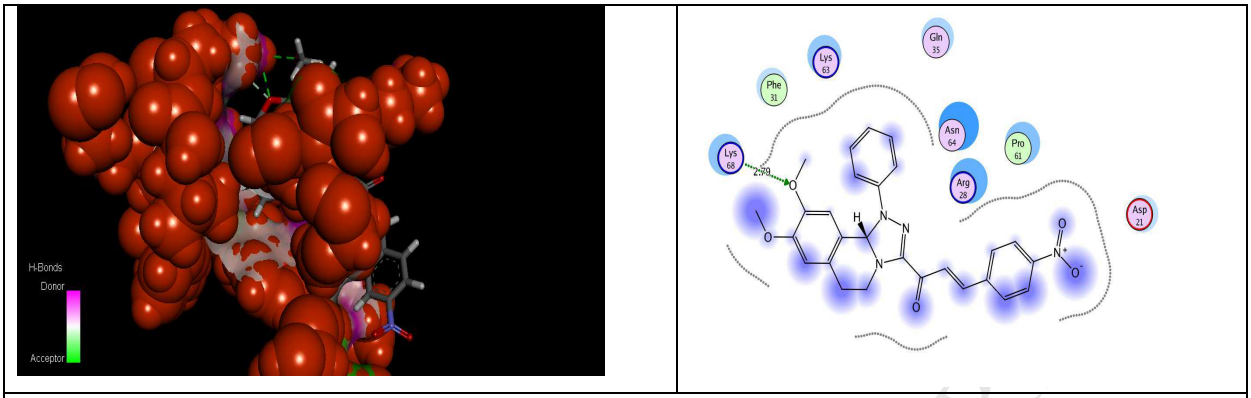

Figure 3: 3D and 2D dimensional representation of compounds **8** and **5** respectively, into the active site of DHFR enzyme.

Real Time Polymerase Chain Reaction

Compounds **5** and **8** were selected from this new series for molecular studies against breast carcinoma as they exhibit excellent cytotoxicity and selectivity toward this cell line. They achieved the lowest IC_{50} values (50.05, 27.15 µg/ml) respectively, (as shown in Table 1) and they were considered safer toward normal melanocytes HFB4. MCF7 cells were treated with IC_{50} values of the two compounds **5** and **8** for 48h at 37°C, then the treated cells plus control were collected for real-time PCR analysis for the following six genes (BAX, P53, Caspase-3, BCL2, CDK4, and MMP1), using specific primers for each one (experimental section). Results in Table 2 demonstrated that compounds **5** and **8** have strongly stimulated apoptotic induction of the human breast carcinoma (MCF7 cells) through induction of the proapoptotic protein BAX with expression values (85,936, and 886,462) relative to their control (33,322). In addition, the tumor suppressor gene p53 was also expressed strongly by the effect of both compounds with expression value (333,111) for compound **5** and (440,272) for compound **8** regarding the expression value of negative control (43,859). With respect to the apoptotic protein Caspase-3, the two compounds showed too potent effect on the expression level of this protein according to data indicated in Table 2. It is clear that compound **8** exhibit better expression values than compound **5** regarding three proteins mentioned above (BAX, P53, and Caspase-3) as showed in the schematic diagram obtained in Figure 4. Finally, the two compounds **5** and **8** decreased strongly the up regulation of antiapoptotic proteins by decreasing BCL2 gene expression to reach (41,723, and 2,635) respectively, compared to untreated MCF7 cells (310,483). Thus, up regulation of p53, BAX, caspase-3 and down regulation of BCL2, MMP1, and CDK4 genes by the two compounds **5** and **8** relative to control promote the apoptotic death of MCF7 cell line.

Table 2: Relative m-RNA transcription of (BAX, P53, Caspase-3, BCL2, CDK4, and MMP1) genes to controls.

Genes	Control	5/MCF7	8/MCF7
BAX	33,322	85,936	886,462
P53	43,859	333,111	440,272
Casp-3	191	364,691	462,065
BCl2	310,483	41,723	2,635
CDK4	442,232	108,685	54,932
MMP1	988,937	330,507	80,798

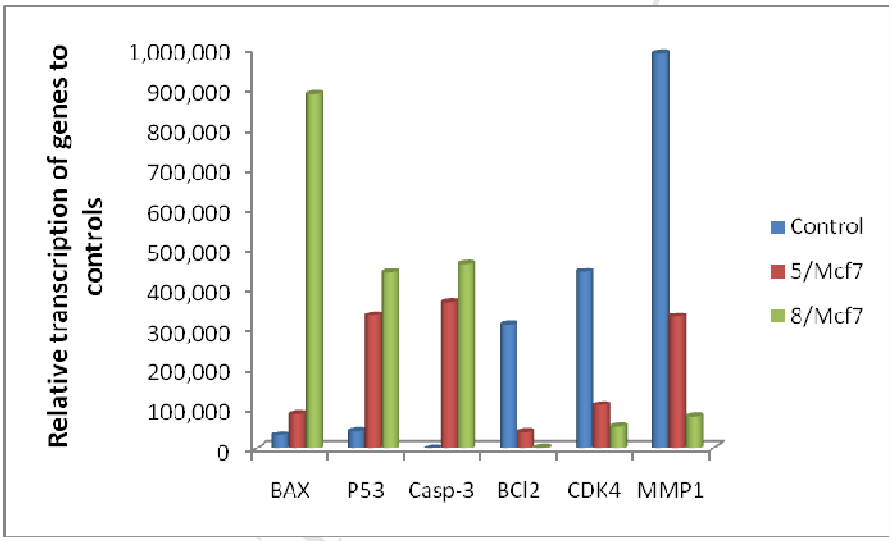

Figure 4: Schematic diagram represented real time PCR data for the following six genes (BAX, P53, Caspase-3, BCL2, CDK4, and MMP1) and their controls.

Flow Cytometer Analysis

Cell cycle analysis was done to detect cell distribution in each phase of cell cycle. The transition from G1 phase to S phase in cell cycle is very important point for controlling cell proliferation. In G1 phase, CDK activity stimulated DNA replication and initiated G1/S transition which committed the cell to divide by inducing genome transcriptional changes [21]. From data obtained in (Table 3, Figure 6), it is noted that both drugs **5** and **8** induced cell growth arrest at G1 phase relative to control sample. This arrest may be due to inactivation of CDK molecule by compound **5** and **8**. Also, it is clear as in Figure 5 that compound **5** and **8** stimulated apoptotic death of breast cell significantly to reach 8.72% and 17.28% respectively, compared to their

control (0.55%). Compound **8** still the most active compound which has strong effect more than compound **5**.

Table 3: The percentage of cell cycle phases and apoptosis of compounds **5** and **8** relative to their control.

Sample code	Conc. (ug/ml)	%G0-G1	%S	%G2-M	%Apoptosis
5/MCF7	50.05 µg/ml	74.52	17.06	0.0	8.72
8/MCF7	27.15 µg/ml	66.11	16.01	0.6	17.28
Cont.MCF7	-	71.13	23.5	4.82	0.55

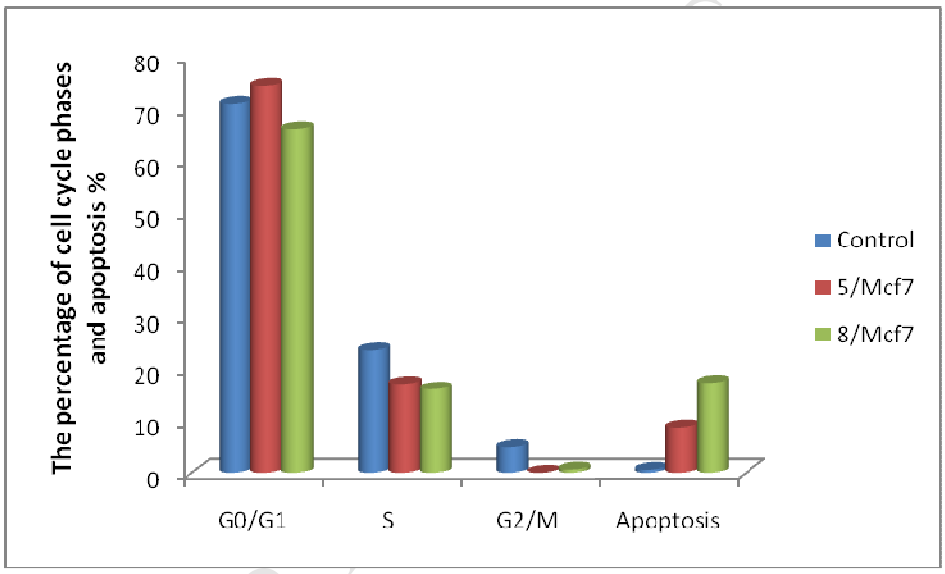

Figure 5: Schematic diagram represented cell cycle analysis and apoptotic results of the two compounds **5** and **8**.

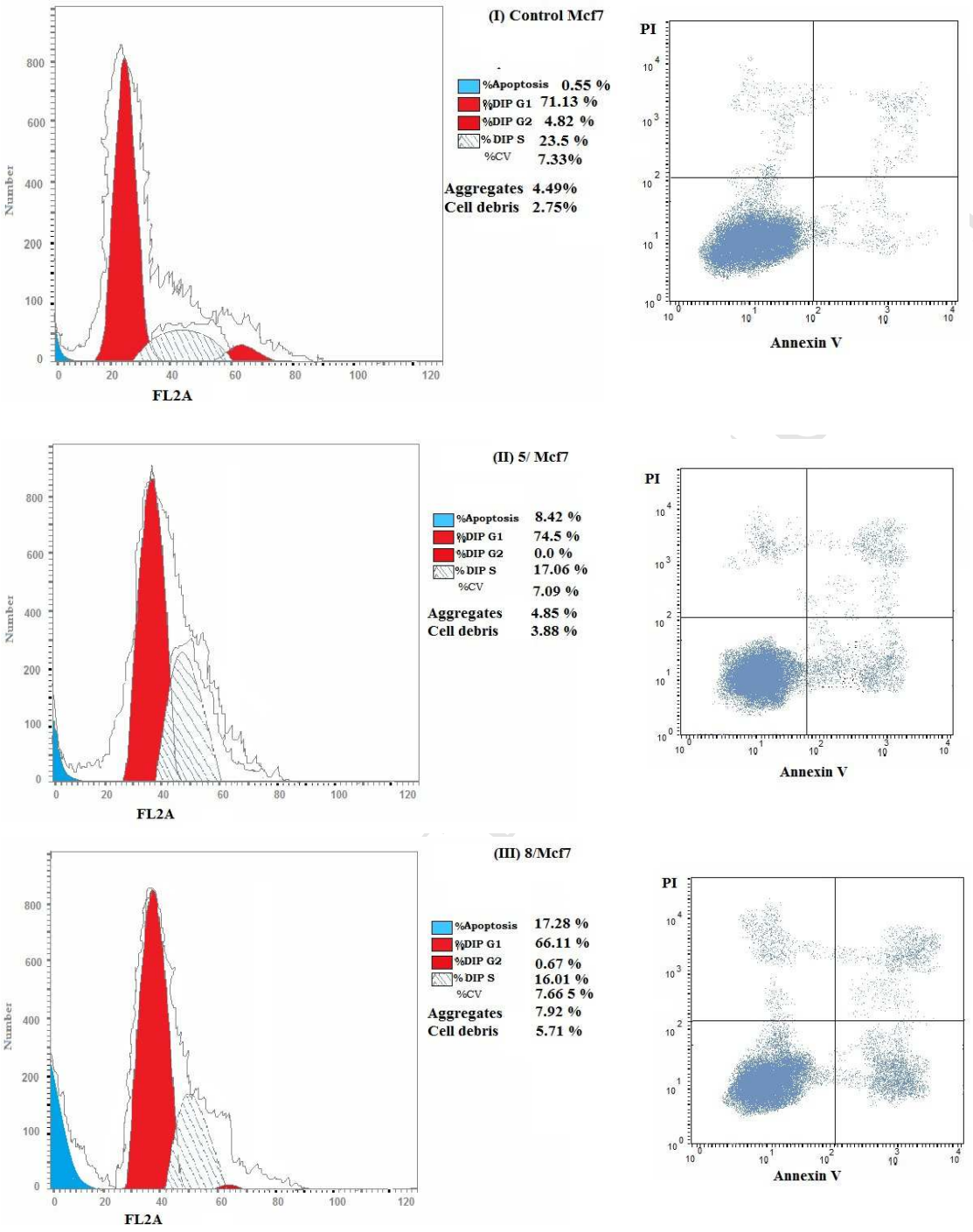

Figure 6: DNA histograms of cell cycle analysis of MCF7 cells after 48 h after treatment with compounds **5** and **8** at their IC_{50} values (50.05 and 27.15 µg/ml), respectively. Cells were stained with propidium iodide and DNA content was then quantified by flow cytometry using the cell quest histogram analysis program. Apoptotic percentage of each sample was determined by (Annexin V-FITC positive). Each histogram was a representative of three independent experiments [11,22].

Elisa for Caspase-3

Cells were grown in RPMI 1640, stimulated with the compounds **5** and **8** to be tested for human active caspase-3 content. The results recorded in Table 4, indicated that apoptotic induction of breast cells was enhanced effectively through activation of caspase-3 by compounds **5** and **8** using Elisa assay. Also, it is noted that compound **8** stimulated caspase-3 activity more effectively than compound **5** as showed in Figure 7.

Table 4: The effect of the two tested novels **5** and **8** on caspase-3 activity.

Cpd. code.	**IC_{50}** (ug/ml)	**OD**	**Caspase3 conc.** (ng/ml)
Compound **8**	27.15	0.706	0.4108
Compound **5**	50.05	0.563	0.3573
Cont. cells (**MCF7**)		0.111	0.0197

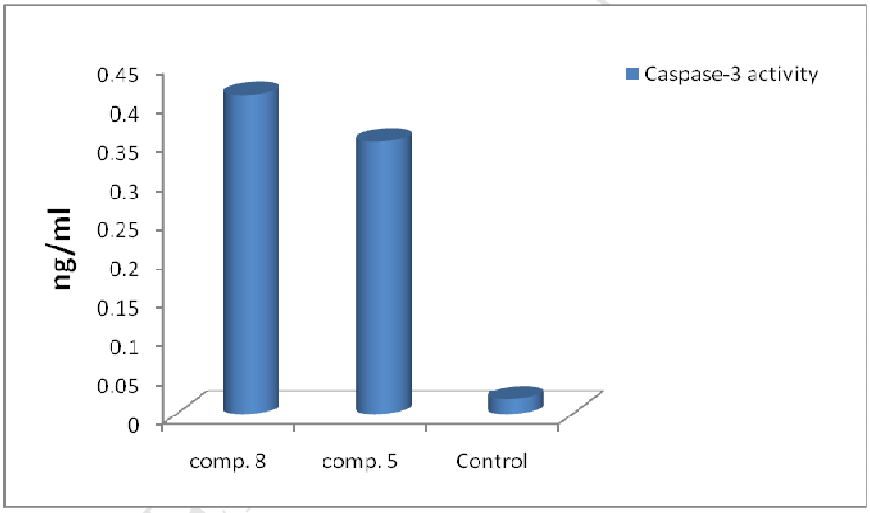

Figure 7: A diagram demonstrated the effect of compounds **5** and **8** regarding apoptotic induction of caspase-3.

Conclusion

Anticancer activity was performed on novel [1,2,4]triazolo[3,4-*a*]isoquinoline chalcones **3-8.** All compounds exhibited strong, moderate and weak effect against all selected cancer cell line. Generally, breast carcinoma revealed higher and promising sensitivity with all derivatives especially compounds **5** and **8** which offered the lowest IC_{50} values (50.05, and 27.15 µg/ml) respectively, relative to the positive control 5-fluorouracil (5-FU) with IC_{50} (178 µg/ml). Compounds **5** and **6** exhibited promising effect with colon carcinoma (114.2, and 187.4 µg/ml)

respectively, compared to their control (201 µg/ml). With respect to hepatocellular carcinoma, all series exhibited the best effect except compound **5** which exhibited moderate effect. Compound **3** recorded strong effect with IC_{50} value (78.13 µg/ml) approximately near to that of 5-FU against lung carcinoma. Compounds **5** and **8** were the best promising and selective anticancer drug especially against breast carcinoma. Also, they exhibited less toxic effect toward human normal melanocytes (HFB4). Theoretical studies proved that compound **8** was considered the most active and promising one. This may be due to the presence of trimethoxy groups which enhance the binding activity of this compound into the active domains 4r3r and 1dls. Real time PCR analysis demonstrated that compounds **5** and **8** have strongly stimulated apoptotic induction of the human breast carcinoma (MCF7 cells) through induction of the pro-apoptotic protein BAX with expression values (85,936, and 886,462) relative to their control (33,322). In addition, the tumor suppressor gene p53 was also expressed strongly by the effect of both compounds with expression value (333,111) for compound **5** and (440,272) for compound **8** regarding the expression value of negative control (43,859). With respect to the apoptotic protein Caspase-3, the two compounds appeared too potent effect on the expression level of this protein. It was appeared that compound **8** exhibited better expression values than compound **5** regarding three proteins mentioned above (BAX, P53, and Caspase-3). The two compounds **5** and **8** decreased strongly the up regulation of antiapoptotic proteins by decreasing BCL2 gene expression to reach (41,723, and 2,635) respectively, compared to untreated MCF7 cells (310,483). Compound **8** down regulated antiapoptotic proteins much more effectively than compound **5**. Flow Cytometer analysis indicated that both compounds cause G1 cell cycle arrest and thus inhibit cell cycle proliferation. Compound **5** and **8** stimulated apoptotic death of breast cell significantly to reach (8.72%, 17.28%) respectively, compared to their control (0.55%). Finally, apoptotic induction of breast cells was enhanced effectively through activation of caspase-3 by compound **8** using Elisa assay.

3. Experimental Part

3.1. Chemistry

Melting points were determined on a Stuart melting point device and they are uncorrected. The ^{1}H and ^{13}C-NMR spectra were recorded in DMSO-d_6 as solvent at 300 MHz and 75MHz, respectively on Varian Gemini NMR spectrometer using TMS as internal standard. Chemical shifts are reported in δ units (ppm). The IR spectra were recorded as KBr using a Bruker-vector 22 spectrophotometer FTIR. Mass spectra were measured on a Shimadzu GMSS -QP-1000 EX mass spectrometer at 70 eV. The elemental analyses were performed at the Microanalytical center, Cairo University.

Synthesis of 1-(8,9-dimethoxy-1-phenyl-1,5,6,10b-tetrahydro-[1,2,4]triazolo[3,4-a]isoquinolin-3-yl)ethan-1-one (1)

To a solution of hydrazonyl halide **i** (5 mmol) and 6,7-dimethoxy-3,4-dihydroisoquinoline **iii** (5 mmo) in tetrahydrofuran (THF) (40 ml) was added triethylamine (TEA) (1.4 ml, 10 mmol) at room temperature. The reaction mixture was refluxed for 8 hours. The mixture was then poured on water and extracted with ethyl acetate. The organic layer was collected, dried over anhydrous sodium sulfate and then filtered. The solvent was evaporated under reduced pressure. The solid product was collected and crystallized from ethanol.

Yield: (70 %) as an orange solid (from ethanol); m.p 130-132 ^{o}C. IR (KBr, cm^{-1}): 1660 (CO); ^{1}H NMR (300 MHz, DMSO-d6): δ, ppm: 2.5 (s, 3H, CH_3), 2.7 (m, 2H, CH_2), 3.6 (s, 3H, OMe), 3.7 (s, 3H, OMe), 4.0 (m, 2H, CH_2), 6.5 (s, 1H, H10b), 6.6 (s, 1H, H7), 6.7 (s, 1H, H10) 6.9-7.4 (m, 5H, Ph-H) MS (EI): m/z = 351 (M^+). Anal. Calcd. for $C_{20}H_{21}N_3O_3$ (351.41): C, 68.36; H, 6.02; N, 11.96. Found: C, 68.56; H, 6.14; N, 11.88.

Synthesis of tetrahydro-[1,2,4]triazolo[3,4-a]isoquinolin-3-yl)-3-arylprop-2-en-1-one (3-8)

A mixture of [1,2,4]triazolo[3,4-*a*]isoquinolin-3-yl)ethan-1-one **1** (0.351 g, 1 mmol) and appropriate aldehydes **2** (1 mmol) was dissolved in 20 mL ethanol. To this mixture, potassium hydroxide (20%, 5 mL) was added at 0–5 ^{o}C. The reaction mixture was stirred at room temperature for 5 h, then poured over ice containing HCl. The yellow solid obtained was then filtered, washed with water and dried. The crude product was crystallized from proper solvent to afford chalcones **3-8**.

(*E*)-1-(8,9-Dimethoxy-1-phenyl-1,5,6,10b-tetrahydro-[1,2,4]triazolo[3,4-*a*]isoquinolin-3-yl)-3-phenylprop-2-en-1-one (3)

Yield: (79 %) as a pale-yellow solid (from ethanol); m.p 134-136 ^{o}C. IR (KBr, cm^{-1}): 1663 (CO); ^{1}H NMR (300 MHz, DMSO-d6): δ, ppm: 2.61-2.82 (m, 2H, H6), 3.41 (s, 3H, OMe), 3.62-3.65 (m, 1H, H5), 3.71 (s, 3H, OMe), 4.22-4.33 (m, 1H, H5), 6.66 (s, 1H, H10b), 6.77 (s, 1H, H7), 6.88-7.15 (m, 2H, H10 and vinyl-H), 7.42-7.67 (m, 11H, Ar-H and vinyl-H) ;^{13}C NMR

(75 MHz, DMSO-d6): δ, ppm: 26.7, 41.3,55.2, 55.4, 77.5, 109, 112.1, 114.8, 120.9, 122.4, 126.9, 128.3, 128.4, 128.8, 129.1, 130.4, 134.3, 141.2, 143.1, 146.9, 148.6, 149.3, 178.8 ; MS (EI): m/z = 439 (M^+). Anal. Calcd. for $C_{27}H_{25}N_3O_3$ (439.52): C, 73.79; H, 5.73; N, 9.56. Found: C, 73.91; H, 5.84; N, 9.72

(*E*)-3-(4-chlorophenyl)-1-(8,9-dimethoxy-1-phenyl-1,5,6,10b-tetrahydro-[1,2,4]triazolo[3,4-*a*]isoquinolin-3-yl)prop-2-en-1-one (4)

Yield: (82 %) as a pale-yellow solid (from ethanol); m.p 184-186 ^oC. IR (KBr, cm^{-1}): 1663 (CO); ^1H NMR (300 MHz, DMSO-d6): δ, ppm: 2.62-2.83 (m, 2H, H6), 3.40 (s, 3H, OMe), 3.61-3.64 (m, 1H, H5), 3.71 (s, 3H, OMe), 4.18-4.34 (m, 1H, H5), 6.65 (s, 1H, H10b), 6.77 (s, 1H, H7) 6.90-7.10 (m, 2H, H10 and vinyl-H), 7.43-7.82 (m, 10H, Ar-H and vinyl-H) ;^{13}C NMR (75 MHz, DMSO-d6): δ, ppm: 26.7, 41.3, 55.2, 55.4, 77.6, 108.9, 111.9, 114.9, 120.5, 121.1, 123.1, 126.9, 128.4, 128.9, 129.2, 130.3, 133.3, 134.9, 139.8, 142.9, 146.9, 148.5, 178.8 ; MS (EI): m/z = 473 (M^+). Anal. Calcd. for $C_{27}H_{24}ClN_3O_3$ (473.96): C, 68.42; H, 5.10; Cl, 7.48; N, 8.87. Found: C, 68.36; H, 5.28; Cl, 7.61; N, 8.62.

(*E*)-1-(8,9-dimethoxy-1-phenyl-1,5,6,10b-tetrahydro-[1,2,4]triazolo[3,4-*a*]isoquinolin-3-yl)-3-(4-nitrophenyl)prop-2-en-1-one (5)

Yield: (89 %) as a pale-yellow solid (from ethanol-dioxane); m.p 195-197 ^oC. IR (KBr, cm^{-1}): 1668 (CO); ^1H NMR (300 MHz, DMSO-d6): δ, ppm: 2.62-2.83 (m, 2H, H6), 3.40 (s, 3H, OMe), 3.68-3.70 (m, 1H, H5), 3.72 (s, 3H, OMe), 4.22-4.33 (m, 1H, H5), 6.66 (s, 1H, H10b), 6.77 (s, 1H, H7), 6.95-7.03 (m, 2H, H10 and vinyl-H), 7.38-8.27 (m, 10H, Ar-H and vinyl-H); MS (EI): m/z = 484 (M^+). Anal. Calcd. for $C_{27}H_{24}N_4O_5$ (484.51): C, 66.93; H, 4.99; N, 11.56. Found: C, 67.13; H, 4.81; N, 11.62

(*E*)-3-(benzo[*d*][1,3]dioxol-5-yl)-1-(8,9-dimethoxy-1-phenyl-1,5,6,10b-tetrahydro-[1,2,4]triazolo[3,4-*a*]isoquinolin-3-yl)prop-2-en-1-one (6)

Yield: (87 %) as a pale-yellow solid (from ethanol); m.p 163-165 ^oC. IR (KBr, cm^{-1}): 1663 (CO); ^1H NMR (300 MHz, DMSO-d6): δ, ppm: 2.61-2.82 (m, 2H, H6), 3.40 (s, 3H, OMe), 3.71 (s, 3H, OMe), 3.67-3.69 (m, 1H, H5), 4.21-4.33 (m, 1H, H5), 6.09 (s, 2H, -OCH_2O-), 6.66 (s, 1H, H10b), 6.77 (s, 1H, H7), 6.93-6.99 (m, 2H, H10 and vinyl-H), 6.96-7.56 (m, 9H, Ar-H and

vinyl-H) ;^{13}C NMR (75 MHz, DMSO-d6): δ, ppm: 26.7, 41.3, 55.2, 55.4, 77.3, 101.5, 106.8, 108.5, 109.0, 112.0, 114.7, 120.5, 120.6, 120.7, 125.2, 127.1, 128.3, 128.8, 129.1, 141.5, 143.2, 146.9, 148.0, 148.5, 149.5, 180.2 ; MS (EI): m/z = 483 (M^+). Anal. Calcd. for $C_{28}H_{25}N_3O_5$ (483.52): C, 69.55; H, 5.21; N, 8.69. Found: C, 69.66; H, 5.29; N, 8.78.

(*E*)-1-(8,9-dimethoxy-1-phenyl-1,5,6,10b-tetrahydro-[1,2,4]triazolo[3,4-*a*]isoquinolin-3-yl)-3-(4-methoxyphenyl)prop-2-en-1-one (7)

Yield: (79 %) as a pale-yellow solid (from ethanol); m.p 182-184 ^{o}C. IR (KBr, cm^{-1}): 1653 (CO); ^{1}H NMR (300 MHz, DMSO-d6): δ, ppm: 2.62-2.83 (m, 2H, H6), 3.41 (s, 3H, OMe), 3.71 (s, 3H, OMe), 3.62-3.80 (m, 1H, H5), 3.81 (s, 3H, OMe), 4.21-4.33 (m, 1H, H5), 6.66 (s, 1H, H10b), 6.77 (s, 1H, H7), 6.93-7.01 (m, 2H, H10 and vinyl-H), 6.98-7.75 (m, 10H, Ar-H and vinyl-H) ;^{13}C NMR (75 MHz, DMSO-d6): δ, ppm: 26.7, 41.3, 55.2, 55.4, 77.3, 109.0, 112.1, 114.4, 114.6, 119.9, 120.7, 126.9, 127.1, 128.3, 129.1, 130.4, 141.4, 143.3, 146.9, 148.5, 149.4, 161.3, 178.9; MS (EI): m/z = 469 (M^+). Anal. Calcd. for $C_{28}H_{27}N_3O_4$ (469.54): C, 71.62; H, 5.80; N, 8.95. Found: C, 71.83; H, 5.93; N, 8.62.

(*E*)-1-(8,9-dimethoxy-1-phenyl-1,5,6,10b-tetrahydro-[1,2,4]triazolo[3,4-*a*]isoquinolin-3-yl)-3-(3,4,5-trimethoxyphenyl)prop-2-en-1-one (8)

Yield: (76 %) as a pale-yellow solid (from ethanol); m.p 143-145 ^{o}C. IR (KBr, cm^{-1}): 1658 (CO); ^{1}H NMR (300 MHz, DMSO-d6): δ, ppm: 2.61-2.82 (m, 2H, H6), 3.42 (s, 3H, OMe), 3.66-3.71 (m, 1H, H5), 3.72 (s, 6H, 2OMe), 3.84 (s, 6H, 2OMe), 4.21-4.33 (m, 1H, H5), 6.65 (s, 1H, H10b), 6.78 (s, 1H, H7), 6.92-6.97 (m, 2H, H10 and vinyl-H), 7.09-7.60 (m, 6H, Ar-H and vinyl-H), 7.61 (s, 2H, Ar-H);^{13}C NMR (75 MHz, DMSO-d6): δ, ppm: 26.7, 41.3, 55.2, 55.4, 55.5, 56.0, 60.0, 77.3, 106.4, 108.9, 112.0, 114.6, 120.7, 120.8, 121.8, 128.3, 129.1, 129.8, 129.9, 141.4, 142.0, 143.3, 146.8, 148.6, 153.0, 179.8 ; MS (EI): m/z = 529 (M^+). Anal. Calcd. for $C_{30}H_{31}N_3O_6$ (529.59): C, 68.04; H, 5.90; N, 7.93. Found: C, 68.23; H, 6.13; N, 7.71.

3.2. Cytotoxicity

Anticancer test was performed using MTT assay, where all instructions were performed typically to our previous work [23]. For this study, all compounds with different concentrations were tested against different humman cell lines as (MCF7, A549. HCT116, Hepg2, and HBF4) for 48h

at 37°C, then all results from l viability test were analyzed using Prism Software program (Graphpad Software incorporated, version 3).

3.3. Docking

All docking and modeling investigations were done according to Salama *et al*. [23] with little modifications using (MOE) program 2009.10 version to predict the ligand protein interactions at the active site. Protein structures of EGFR and DHFR were downloaded from the PDB data bank (http://www.rcsb.org/ - PDB codes: 4r3r, and 1DLS) respectively. The two proteins were prepared for the modeling by the following instructions. The standard ligand molecules were removed from the active site of the protein, then addition of hydrogen atoms was performed to the proteins and keeping all the heavy atoms fixed until RMS gradient of 0.01 kcal mol^{-1} and RMS distance of 0.1 Å were reached. Partial charges were computed using MMFF94x force field. The structures were subjected to energy minimization using MMFF94x force field and the partial charges were computed using the same force field. At the end of this program, the final data was visualized through BIOVIA Discovery Studio V6.1.0.15350, where the target molecule simulation results with the active domains were saved as pdb version.

3.4. PCR Analysis

Real time polymerase chain reaction (qPCR) was performed using Qiagen RNA extraction/SIGMA PCR kit and Rotor gene PCR system as reader. All steps were done according to Ali et al.,[24]. Total RNA was extracted from compound **5** and **8** treated MCF7 and from their control. The purity and yield of obtained RNA were recorded spectrophotometrically. Then highly reproducible cDNA strands and subsequent PCR test were performed in a single tube. The perfect primer pairs were selected for the tested genes (BAX, BCL2, P53, Casp-3, CDK4, MMP1) and for housekeeping gene (GAPDH) where, GC content not exceeded 60% and Tm range was (55-60 °C). Primers sequence were as follow: Sense BAX (5'-TTC CGA GTG GCA GCT GAG ATG TTT-3') and antisense BAX (5'-TGC TGG CAA AGT AGA AGA GGG CAA-3'), Sense BCL2 (5'-CAT GCC AAG AGG GAA ACA CCA GAA-3') and antisense BCL2 (5'-GTG CTT TGC ATT CTT GGA TGA GGG-3'), sense P53 (5'-GCCCAACAACACCAGCTCCT -3') and antisense P53(5'-CCTGGGCATCCTTGAGTTCC-3'), Casp-3 sense (5'-TTC ATT ATT CAG GCC TGC CGA GG-3'), and antisense Casp-3 (5'-TTC TGA CAG GCC ATG TCA TCC TCA-3'), sense CDK4 (5′-TCGAAAGCCTCTCTTCTGTG-3′) and antisense CDK4 (5′-TACATCTCGAGGCCAGTCAT-3′), and finally sense MMP1(5′-ctggccacaactgccaaatg-3′) and antisense MMP1 (5′-ctgtccctgaacagcccagtactta-3′). After the run, the results were expressed in Cycle threshold (Ct). Relative quantitation of each tested gene was assessed according to the calculation of delta-delta Ct [24].

3.5. Flow Cytometer Analysis

Cell cycle analysis was carried out according to our previous study done by Magda F. Mohamed *et al,.* [25]. to detect the cell cycle distribution using Ab139418 kit for quantitation of DNA content in MCF7 cultured cells (treated (with compound 5 and 8) and non treated) using propidium iodide stain then flow cytometry analysis was followed up. Also the percentage of apoptosis was recorded.

3.6. Elisa for Caspase-3

ELISA for caspase-3 was done according to Ayat G Ali et al., [24] using (The Max Discovery™ Caspase-3 Colorimetric Detection Kit Manual (cat. no # 5811)) and cells were obtained from American Type Culture Collection, cells were grown in RPMI 1640 containing 10% fetal bovine serum at 37°C, stimulated with the compounds **5** and **8** to be tested for caspase3, and lysed with cell extraction buffer. This lysate was diluted in Standard Diluent Buffer over the range of the assay and measured for human active caspase-3 content. (cells are Plated in a density of 1.2 – 1.8 × 10,000 cells/well in a volume of 100µl complete growth medium + 100 ul of the tested compound per well in a 96-well plate for 24 hours before the enzyme assay for Tubulin.)

References:

[1] C.-N. Lin, H.-K. Hsieh, H.-H. Ko, M.-F. Hsu, H.-C. Lin, Y.-L. Chang, M.-I. Chung, J.-J. Kang, J.-P. Wang, C.-M. Teng, Chalcones as potent antiplatelet agents and calcium channel blockers, Drug Dev. Res. 53 (2001) 9–14. doi:10.1002/ddr.1163.

[2] J.C. Onyilagha, B. Malhotra, M. Elder, C.J. French, G.H.N. Towers, Comparative studies of inhibitory activities of chalcones on tomato ringspot virus (ToRSV), Can. J. Plant Pathol. 19 (1997) 133–137. doi:10.1080/07060669709500541.

[3] H.-K. Hsieh, L.-T. Tsao, J.-P. Wang, C.-N. Lin, Synthesis and anti-inflammatory effect of chalcones, J. Pharm. Pharmacol. 52 (2000) 163–171. doi:10.1211/0022357001773814.

[4] B.P. Bandgar, S.S. Gawande, R.G. Bodade, N.M. Gawande, C.N. Khobragade, Synthesis and biological evaluation of a novel series of pyrazole chalcones as anti-inflammatory, antioxidant and antimicrobial agents, Bioorg. Med. Chem. 17 (2009) 8168–8173. doi:10.1016/j.bmc.2009.10.035.

[5] A.A. Bekhit, T. Abdel-Aziem, Design, synthesis and biological evaluation of some pyrazole derivatives as anti-inflammatory-antimicrobial agents, Bioorg. Med. Chem. 12 (2004) 1935–1945. doi:10.1016/j.bmc.2004.01.037.

[6] R. Li, G.L. Kenyon, F.E. Cohen, X. Chen, B. Gong, J.N. Dominguez, E. Davidson, G. Kurzban, R.E. Miller, E.O. Nuzum, P.J. Rosenthal, J.H. McKerrow, In vitro antimalarial activity of chalcones and their derivatives, J. Med. Chem. 38 (1995) 5031–5037. doi:10.1021/jm00026a010.

[7] A.M. Asiri, S.A. Khan, Synthesis and anti-bacterial activities of a bis-chalcone derived from thiophene and its bis-cyclized products, Molecules. 16 (2011) 523–531. doi:10.3390/molecules16010523.

[8] M.F. Mohamed, M.S. Mohamed, S. a Shouman, M.M. Fathi, I.A. Abdelhamid, Synthesis and biological evaluation of a novel series of chalcones incorporated pyrazole moiety as anticancer and antimicrobial agents., Appl. Biochem. Biotechnol. 168 (2012) 1153–62. doi:10.1007/s12010-012-9848-8.

[9] M.R. Heidari, A. Foroumadi, A. Amirabadi, A. Samzadeh-Kermani, B.S. Azimzadeh, A. Eskandarizadeh, Evaluation of anti-inflammatory and analgesic activity of a novel rigid 3, 4-dihydroxy chalcone in mice, Ann. N. Y. Acad. Sci. 1171 (2009) 399–406. doi:10.1111/j.1749-6632.2009.04904.x.

[10] S. Shenvi, K. Kumar, K.S. Hatti, K. Rijesh, L. Diwakar, G.C. Reddy, Synthesis, anticancer and antioxidant activities of 2,4,5-trimethoxy chalcones and analogues from asaronaldehyde: Structure–activity relationship, Eur. J. Med. Chem. 62 (2013) 435–442. doi:10.1016/j.ejmech.2013.01.018.

[11] M.F. Mohamed, M.S. Mohamed, M.M. Fathi, S.A. Shouman, I.A. Abdelhamid, Chalcones incorporated pyrazole ring inhibit proliferation , cell cycle progression , angiogenesis and induce apoptosis of MCF7 cell line, Anticancer Agents Med Chem. 14 (2014) 1282–1292.

[12] K. V Sashidhara, A. Kumar, M. Kumar, J. Sarkar, S. Sinha, Synthesis and in vitro evaluation of novel coumarin-chalcone hybrids as potential anticancer agents., Bioorg. Med. Chem. Lett. 20 (2010) 7205–11. doi:10.1016/j.bmcl.2010.10.116.

[13] N.M. Elwan, H.A. Abdelhadi, T.A. Abdallah, H.M. Hassaneen, Synthesis of [1,2,4]triazolo[3,4-a]isoquinolines and pyrrolo[2,1-a]isoquinolines using α-keto hydrazonoyl halides, Tetrahedron. 52 (1996) 3451–3456. doi:10.1016/0040-4020(96)00024-5.

[14] C.-C. Lee, H.-Y. Shiao, W.-C. Wang, H.-P. Hsieh, Small-molecule EGFR tyrosine kinase inhibitors for the treatment of cancer, Expert Opin. Investig. Drugs. 23 (2014) 1333–1348. doi:10.1517/13543784.2014.928283.

[15] A. Lluch, P. Eroles, J.-A. Perez-Fidalgo, Emerging EGFR antagonists for breast cancer, Expert Opin. Emerg. Drugs. 19 (2014) 165–181. doi:10.1517/14728214.2014.903919.

[16] S. Noda, S. Kanda, Addressing epidermal growth factor receptor tyrosine kinase inhibitor resistance in non-small cell lung cancer, Expert Rev. Respir. Med. 10 (2016) 547–556. doi:10.1586/17476348.2016.1164603.

[17] P. Seshacharyulu, M.P. Ponnusamy, D. Haridas, M. Jain, A.K. Ganti, S.K. Batra, Targeting the EGFR signaling pathway in cancer therapy, Expert Opin. Ther. Targets. 16 (2012) 15–31. doi:10.1517/14728222.2011.648617.

[18] L. Yamini, M. Vijjulatha, Inhibitors of human dihydrofolate reductase: A computational

design and docking studies using glide, E-Journal Chem. 5 (2008) 263–270. doi:10.1155/2008/401738.

[19] H.M. Hassaneen, H.M.E. Hassaneen, Y.S. Mohammed, R.M. Pagni, Synthesis, Reactions and Antibacterial Activity of 3-Acetyl[1,2,4]triazolo[3,4-a]isoquinoline Derivatives using Chitosan as Heterogeneous Catalyst under Microwave Irradiation, Zeitschrift Für Naturforsch. B. 66 (2011) 299–310. doi:10.1515/znb-2011-0313.

[20] V. Srivastava, A.S. Negi, J.K. Kumar, U. Faridi, B.S. Sisodia, M.P. Darokar, S. Luqman, S.P.S. Khanuja, Synthesis of 1-(3′,4′,5′-trimethoxy) phenyl naphtho[2,1b]furan as a novel anticancer agent, Bioorg. Med. Chem. Lett. 16 (2006) 911–914. doi:10.1016/j.bmcl.2005.10.105.

[21] C. Bertoli, J.M. Skotheim, R.A.M. de Bruin, Control of cell cycle transcription during G1 and S phases, Nat Rev Mol Cell Biol. 14 (2013) 518–528. doi:10.1038/nrm3629.

[22] TACS Annexin V-FITC Apoptosis Detection Kit 4830-01-K: R&D Systems, (2010).

[23] S.K. Salama, M.F. Mohamed, A.F. Darweesh, A.H.M. Elwahy, I.A. Abdelhamid, Bioorganic Chemistry Molecular docking simulation and anticancer assessment on human breast carcinoma cell line using novel bis (1 , 4-dihydropyrano [2 , 3- c], Bioorg. Chem. 71 (2017) 19–29. doi:10.1016/j.bioorg.2017.01.009.

[24] A.G. Ali, M.F. Mohamed, A.O. Abdelhamid, M.S. Mohamed, A novel adamantane thiadiazole derivative induces mitochondria-mediated apoptosis in lung carcinoma cell line, Bioorg. Med. Chem. 25 (2017) 241–253. doi:10.1016/j.bmc.2016.10.040.

[25] M.F. Mohamed, A.F. Darweesh, A.H.M. Elwahy, I.A. Abdelhamid, Synthesis, characterization and antitumor activity of novel tetrapodal 1,4-dihydropyridines: p53 induction, cell cycle arrest and low damage effect on normal cells induced by genotoxic factor H2O2, RSC Adv. 6 (2016) 40900–40910. doi:10.1039/C6RA04974E.

Highlights

Tetrahydro-[1,2,4]triazolo[3,4-a]isoquinoline

Chalcones.

Breast cancer

Modeling docking study

Apoptosis

Cell cycle arrest